Tribology of MoS_2-Based Nanocomposites

Kunhong Hu, Xianguo Hu, Yufu Xu, Xiaojun Sun and Yang Jiang

Abstract In this chapter, the preparation and tribological properties of MoS_2-based nanocomposites were reviewed, including nanocomposites of MoS_2 with different morphologies, MoS_2/inorganic compound nanocomposites, MoS_2/polymer nanocomposites, and Ni–P–(nano-MoS_2) composite coatings. The nanocomposites of MoS_2 can be prepared by mechanical-mixing two kinds of nano-MoS_2 with different morphologies or chemically synthesizing from sodium molybdate and different sulfides. The nanocomposites of MoS_2 reveal better tribological properties than their original materials. Moreover, the chemical method presents advantages over the mechanical one in the preparation of the MoS_2 nanocomposites with different morphologies for lubrication applications. Using an appropriate chemical method may produce MoS_2/inorganic compound nanocomposites such as MoS_2/TiO_2 nanocomposite. Two kinds of nanoparticles (nano-MoS_2 and nano-TiO_2) reveal a synergistic effect on the tribological properties of the MoS_2/TiO_2 nanocomposite. MoS_2/polymer nanocomposites may be prepared by adding nanosized MoS_2 into polymers or using the chemical intercalation technology. The chemical intercalation technology may lead to disperse MoS_2 into polymer matrix better than the mechanical-filled way. However, the intercalation compound of MoS_2/polymer can not present a satisfactory lubrication performance, because the intercalation process destroys the 2H structure of MoS_2 with better lubricity. The Ni–P coatings may be co-deposited with nanosized MoS_2 on medium carbon steel substrate by electroless plating. The

K. Hu (✉)
Department of Chemical and Materials Engineering, Hefei University,
Hefei 230601, People's Republic of China
e-mail: hukunhong@163.com

X. Hu (✉) · Y. Xu
Institute of Tribology, Hefei University of Technology, Hefei 230009,
People's Republic of China
e-mail: xghu@hfut.edu.cn

X. Sun
Stat Key Laboratory, Lanzhou Institute of Chemical Physics, Chinese Academy of Sciences,
Lanzhou 730000, People's Republic of China

Y. Jiang
School of Materials Science and Enginering, Hefei University of Technology,
Hefei 230009, People's Republic of China

J. Paulo Davim (ed.), *Tribology of Nanocomposites*, Materials Forming,
Machining and Tribology, DOI: 10.1007/978-3-642-33882-3_3,

obtained Ni–P–nano-MoS_2 composite coating shows an excellent lubricating performance. The present review concluded the synthesis and tribological applications of MoS_2-based nanocomposite well.

1 Introduction

Nanocomposites have wide applications in modern materials science and nanotechnology. Recently, the significance of nanocomposites in tribology was also paid so much attention. The nanocomposites may be prepared by mechanical mixing, chemical synthesis and coating technology. The components in a nanocomposite may offset their defects and enhance their merits mutually. Thus, the nanocomposites usually have better performances in friction reduction and wear resistance than their original materials. Some solid lubricants, such as molybdenum disulfide (MoS_2), graphite, and carbon nanotube, are often used as materials to synthesize nanocomposites. Herein, several selected features concerning the MoS_2-based nanocomposites were reviewed based on our recent researches and results reported by other researchers. In the second section, the structure and properties of bulk 2H-MoS_2 were reviewed. Section 3 describes the development in nanosized MoS_2 (nano-MoS_2). Section 4 is focused on the synthesis and tribological properties of MoS_2-based nanocomposites, including MoS_2 nanocomposites with different morphologies, MoS_2/inorganic compound nanocomposites, MoS_2/polymer nanocomposites, and Ni–P–(nano-MoS_2) composite coatings.

2 Molybdenum Disulfide

Molybdenum disulfide (MoS_2) is the main component of molybdenite that is the principal ore of molybdenum. MoS_2 has three crystal states, i.e. 1T, 2H, and 3R [1]. The 2H layered crystal structure is usually considered as the most important factor for lubrication of MoS_2. The commercial lubricant of bulk 2H-MoS_2 presents a platelet-like shape (Fig. 1) [2]. The bulk 2H-MoS_2 is composed of layered structures that contains strong S–Mo–S covalent bonds in inside layers and weak Van der Waals gaps between molecular layers. The 2H layered structure results in a strong (002) peak in the powder X-ray diffraction pattern (XRD) of MoS_2 (Fig. 2) [3].

The Van der Waals gaps between MoS_2 layers are easy to slide under the friction shearing (Fig. 3). In addition, S atoms on MoS_2 have an intensive adsorption effect on the metal surface. The two characteristics may provide persistent lubrication for metal friction pairs, especially in extreme environments such as high-temperature and high-vacuum [4, 5]. Thus, MoS_2 has become an important solid lubricant in aviation and aerospace. Moreover, MoS_2 is also a known-well additive in lubricating oils, polymers, and coatings [1, 6, 7].

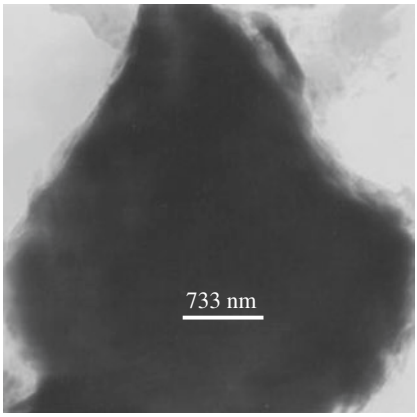

Fig. 1 TEM image of 2H-MoS2 (adapted from Ref. [2])

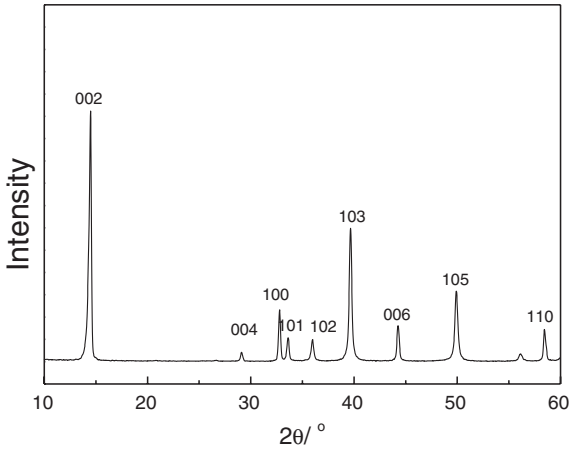

Fig. 2 X-ray diffraction pattern of 2H-MoS_2 powder (adapted from Ref. [3])

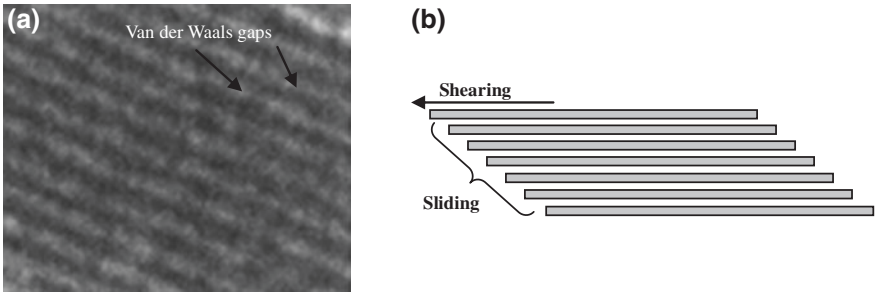

Fig. 3 Van der Waals gaps between MoS_2 layers (**a**) and schematic diagram of their shearing-sliding (**b**)

3 Nanosized Molybdenum Disulfide

Nano-MoS_2 usually presents better lubrication performance than bulk MoS_2. Thus, considerable attention has been given to nano-MoS_2. There has been a lot of researches on the synthesis [8–13] and tribology of nano-MoS_2 [14–26]. The chemical routes to synthesize nano-MoS_2 include gas phase growth [8], hydrothermal or solvothermal synthesis [10], decomposition of precursors [11, 12], etc. The synthesized nano-MoS_2 involves tube-like [8, 9], platelet-like [11], sphere-like [12] and fullerene-like [8] shapes. The morphologies of nano-MoS_2 can be categorized into two: layer-opened and layer-closed.

The layer-opened MoS_2, such as platelet-like nano-MoS_2 (MoS_2 nano-platelet), contains basal surfaces and rim-edge surfaces [27]. The atoms on the rim-edge surface have high chemical activity. The chemically active MoS_2 nano-platelet is easy oxidized during friction process. The oxidation resultants, such as MoO_3 and sulfates, may function as a lubrication film to reduce friction [28, 29]. However, an excessive oxidation can also weaken the lubrication of nano-platelet. Because MoS_2 nano-platelet has a similar 2H layered structure to that of the bulk MoS_2, its lubrication may also be explained using the easy sliding between S–Mo–S molecular layers [23].

Forming layer-closed structures, such as inorganic fullerene-like, tube-like and hollow sphere-like, may eliminate the active rim-edge surface and increase the chemical stability of nano-MoS_2 [2, 15, 16, 23]. The oxidation film is not the main reason for the excellent tribological properties of the layer-closed nano-MoS_2. The chemical stability enables the layer-closed nano-MoS_2 to function as lubrication well during friction process. Moreover, the lubrication mechanism of the layer-closed nano-MoS_2 was also attributed to elastic deformation and exfoliation of MoS_2 and the delivery of the exfoliated nano-sheets to the contact area [14, 15, 24, 30, 31], which have been observed through advanced characterization technologies [25, 26]. Due to the particular lubrication mechanism, the layer-closed nano-MoS_2 can usually reveal very excellent tribological properties.

Recently, the morphological effect on the tribological properties of MoS_2 was studied in liquid paraffin (LP) and rapeseed oil. The layer-closed MoS_2 nano-spheres had a better lubrication performance than the layer-opened MoS_2 nano-platelets at a content of 1.5 wt % in liquid paraffin, but a worse one at 0.5 wt % [23]. However, the layer-closed nano-sphere revealed considerable advantages over the layer-opened one in rapeseed oil at any of content used (unpublished results).

4 Molybdenum Disulfide Nanocomposites

4.1 MoS_2 Nanocomposites with Different Morphologies

Three kinds of MoS_2, namely, micro-platelet (325 meshes), hollow nano-sphere, and nano-platelet, were used to prepare MoS_2 nanocomposites with different morphologies by mechanical mixing [32]. The diameters of MoS_2 hollow

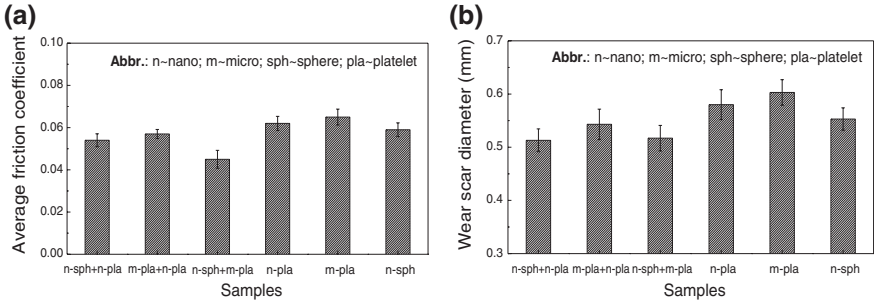

Fig. 4 Tribological properties of MoS_2 nanocomposites prepared by mechanical mixing (adapted from Ref. [32])

nano-spheres vary from 80 to 200 nm with an about 15 nm shell. The thickness of nano-platelet is about 7 nm and the length about 40 nm. Some composites were obtained by proportionally mixing any two of the three kinds of MoS_2 in liquid paraffin.

Figure 4 provides results of four-ball tribological tests for the 1.5 wt % MoS_2 nanocomposites in liquid paraffin [32]. The tests were conducted at 1450 rpm and 300 N for 30 min. Figure 4a shows the average friction coefficients of different nanocomposites. The pure MoS_2 nano-spheres presented better anti-friction performance in liquid paraffin than the two pure platelets-like MoS_2. However, the MoS_2 nanocomposites had lower friction coefficients than that of the pure MoS_2 nano-spheres in liquid paraffin. The lowest friction coefficient occurred in the LP sample with the nano-sphere/micro-platelet composite (20 wt % nano-spheres and 80 wt % micro-platelets). Thus, forming nanocomposites may improve the anti-friction performance of MoS_2.

Figure 4b provides the anti-wear results (average wear scar diameter) of four-ball tests. As shown in the figure, The LP sample with MoS_2 nano-spheres presented better anti-wear properties than that with MoS_2 micro-platelets or nano-platelets. Some of LP samples with the nanocomposites presented better anti-wear performances than that with any of the three pure MoS_2. The nano-sphere/nano-platelet nanocomposite (60 wt % nano-spheres and 40 wt % micro-platelets) presented the best anti-wear performance.

These mentioned above indicate that the morphology of MoS_2 has an influence on the tribological properties of MoS_2 nanocomposites. The nanocomposites of MoS_2 with different morphologies may improve the wear resistance and friction reduction of LP more than any of the three morphologies of MoS_2 singly did. The different tribological properties of the three kinds of MoS_2 were attributed to their different lubrication mechanisms. The lubrication mechanism of bulk MoS_2 is associated with the sliding between molecular layers induced by the friction shearing. With a similar layered structure to that of bulk 2H-MoS_2, MoS_2 nano-platelets may also present the shearing and sliding lubrication mechanism (Fig. 5a) [23].

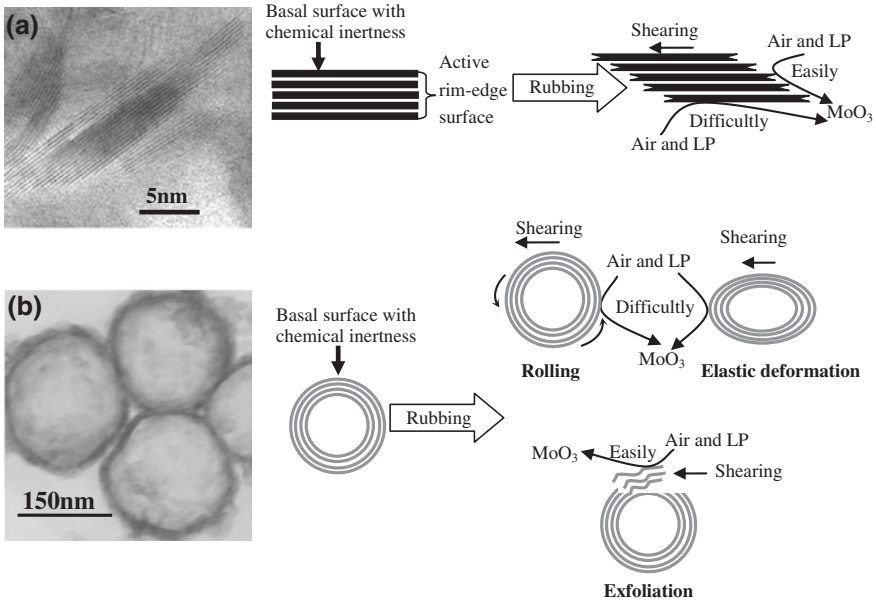

Fig. 5 Schematic of lubrication-wear mechanism of **a** MoS_2 nano-platelet and **b** MoS_2 nano-sphere (adapted from Ref. [23])

The excellent tribological properties of spherical nano-MoS_2 may be explained by its chemical inertness, rolling friction, deformation, and exfoliation-delivery of MoS_2 sheets to the contact area (Fig. 5b).

According the results of Stribeck curves [23], the rotation speed used (1450 rpm) fell in the end of the mixed lubrication. Thus, the oil film thickness between the friction pairs should be slightly larger than the surface roughness of friction pairs (0.032 μm). The MoS_2 nano-platelets with the smallest sizes easily penetrated into the friction contact region to function as lubrication. However, it was easy for the active nano-platelets to be excessively oxidized into MoO_3 (Fig. 5a). Thus, the nano-platelets didn't present better lubrication properties than the nano-spheres.

The better tribological properties of the nanocomposites resulted from the cooperation between two different lubrication mechanisms [32]. The size of the bulk MoS_2 micro-platelets exceeded the thickness of the oil film between the friction pairs. The adsorbed micro-platelets mainly functioned as a separation body between the friction pairs. Thus, the thickness of the oil film was magnified. The nano-MoS_2, i.e. nano-sphere or nano-platelet, was easier to penetrate into the contact region (Fig. 6a). When the micro-platelets adsorbed were worn by the friction shearing, the size of micro-platelet was close to the thickness of oil film. Then it occurred that the cooperation between the shearing-sliding of 2H structure and the rolling-deformation-exfoliation of nano-spheres (Fig. 6b). The similar cooperation

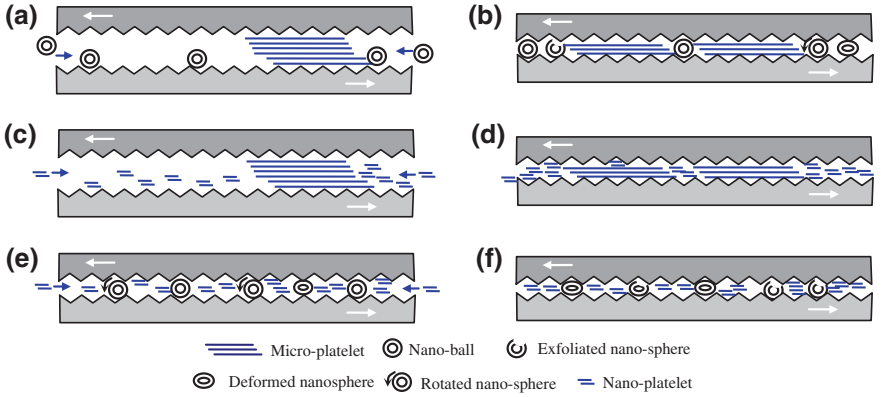

Fig. 6 Schematic of the synergistic lubrication between two kinds of MoS_2 particles: **a** initial stage and **b** stable stage lubricated by nano-spheres and micro-platelet, **c** initial stage and **d** stable stage lubricated by nano-platelets and micro-platelet, **e** initial stage and **f** stable stage slices lubricated by nano-spheres and nano-platelets (adapted from Ref. [32])

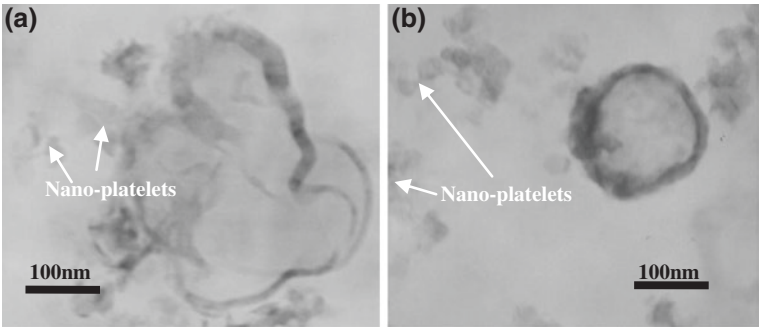

Fig. 7 TEM images of MoS_2 nanocomposite synthesized at a molar ratio (Na_2S to CH_3CSNH_2) of: **a** 1:2 and **b** 1:4 (adapted from Ref. [34])

was observed between nano-platelet and micro platelet or nano-sphere and nano-platelet (Figs. 6c–f).

MoS_3 may be synthesized using the reaction of sulfides and sodium molydate. Nano-MoS_2 can be obtained after heating MoS_3 in H_2 or N_2. The morphology of nano-MoS_2 is affected by the sulfides used [11, 33]. CH_3CSNH_2 (TAA) may produce spherical nano-MoS_2 while Na_2S platelet-like one. It was possible to prepare MoS_2 nanocomposite with different morphologies by adjusting the proportion of the two sulfides [34]. However, Na_2S can disturb the forming processes of nano-spheres especially at low dosages of TAA (Fig. 7a). The nano-sphere/nano-platelet composite can be obtained only at high TAA dosages (Fig. 7a). The Schematic of forming MoS_2 nanocomposite was shown in Fig. 8.

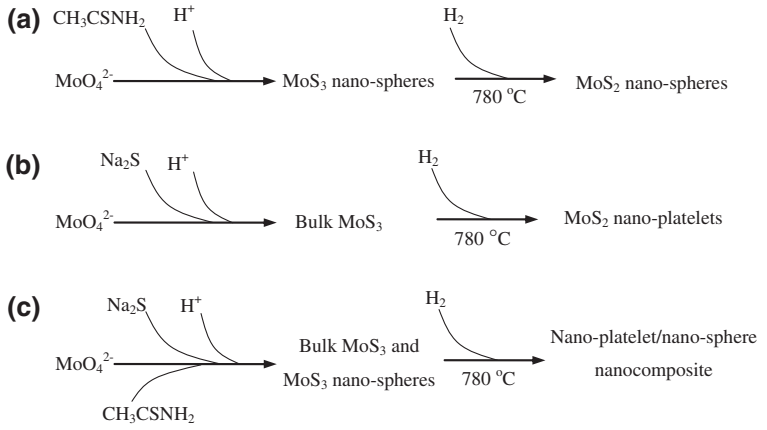

Fig. 8 Schematic of forming nano-MoS_2: **a** nano-spheres, **b** nano-platelets, and **c** MoS_2 nanocomposite with different morphologies (adapted from Ref. [34])

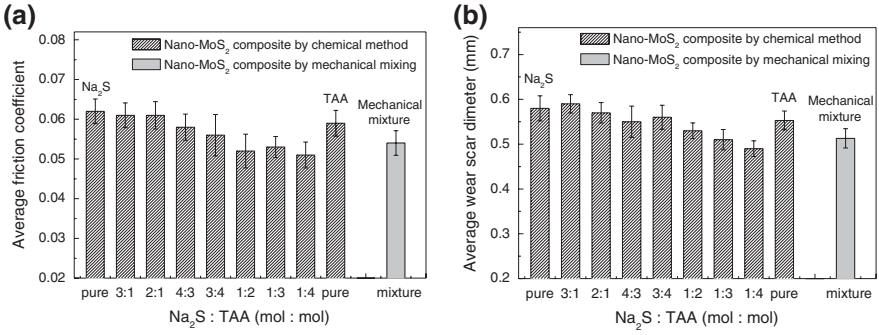

Fig. 9 Variations of friction coefficient (**a**) and wear scar diameter (**b**) lubricated by liquid paraffin with MoS_2 nanocomposites (adapted from Ref. [34])

Figure 9 shows the four-ball tribological properties of the MoS_2 nanocomposite at a rotating speed of 1450 rpm and a constant load of 300 N in liquid paraffin [34]. Figure 9a is the effect of the molar ratio of Na_2S to TAA on the average friction coefficient. As shown in the figure, the LP sample presented the lowest friction coefficient (0.051) at the proportion of 1:4 (Na_2S to TAA). Figure 9b confirms that the variation of AWSD was approximately correlated to the change in friction coefficients. The steel balls lubricated by liquid paraffin with the 1:4 nano-sphere/nano-platelet composite also presented the lowest AWSD (0.49 mm). Compared with the nanocomposites prepared by the mechanically mixing method, the chemically synthesized MoS_2 nanocomposite presented better tribological properties. The chemical method could mix nano-spheres and

nano-platelets better than the mechanical one. Thus, the MoS_2 nanocomposite by chemical method showed better tribological properties. However, the difference between the two mixing method is not very obvious. This is mainly because that Na_2S disturbed the forming of nano-sphere.

4.2 MoS_2/Inorganic Compound Nanocomposites

A MoS_3/TiO_2 composite was synthesized by quickly depositing MoS_3 on TiO_2 under a strong acidic solution [35]. Calcining the MoS_3/TiO_2 composite at 450 °C in H_2 led to a MoS_2/TiO_2 nanocomposite. The MoS_2/TiO_2 nanocomposite of 6:5 (wt:wt) was characterized in the literauture. The XRD pattern in Fig. 10a is consistent with that in JCPDS89-4921 belonging to the anatase TiO_2. All diffraction peaks of anatase TiO_2 were still present in the XRD pattern of the MoS_2/TiO_2 nanocomposite (Fig. 10b), indicating that the anatase nano-TiO_2 was not destroyed during the synthesis process. The diffraction peaks of pure nano-MoS_2, reported in Ref. [20], were found in the XRD pattern of the nanocomposite. As shown in Fig. 11a, b, nano-MoS_2 particles were distributed among TiO_2 particles, composed of typical layered structures with an average length of about 15 nm (10–20 nm) and an average thickness of about 5 nm. The nano-MoS_2 particles in the nanocomposite have larger layer distances (~0.66 nm) as compared with pure nano-MoS_2. The findings confirm that the MoS_2/TiO_2 nanocomposite was successfully prepared and provide a new method to synthesize MoS_2-based nanocomposites.

$$3S^{2^-} + MoO_4^{2^-} + 8H^+ + TiO_2 \longrightarrow MoS_3/TiO_2 \downarrow + 4H_2O.$$

$$MoS_3/TiO_2 + H_2 \xrightarrow{450\,^\circ C/30\ min} \text{nano} - MoS_2/TiO_2 + H_2S.$$

The tribological properties of MoS_2/TiO_2 nanocomposite were investigated in liquid paraffin on a four-ball tribometer at 0.556 m/s under 300 N [36]. The MoS_2/TiO_2 nanocomposite was found to be a promising lubricant additive with a better performance than either nano-MoS_2 or nano-TiO_2 alone. Figure 12a provides the variation in average friction coefficient with the mass ratio of MoS_2 to TiO_2 in the nanocomposite. The pure nano-TiO_2 shows the highest friction coefficient and is not an appropriate anti-friction additive in LP. The lowest friction coefficient was observed in the nanocomposite of 2:1 (MoS_2:TiO_2). Figure 12b shows the variation in AWSD with the mass ratio of MoS_2 to TiO_2 in the nanocomposite. The best anti-wear performance was found in the nanocomposite of 4:1. The nanocomposite of 2:1 led to the lowest friction coefficient but an AWSD close to that of pure nano-MoS_2. These mentioned above indicate that forming MoS_2/TiO_2 nanocomposite improved the tribological properties of MoS_2.

Abrasive wear was a main wear factor of steel balls lubricated by LP with the MoS_2/TiO_2 nanocomposite. The nanocomposite, containing higher chemical activity and smaller sizes, could penetrate through the oil film to the contact region.

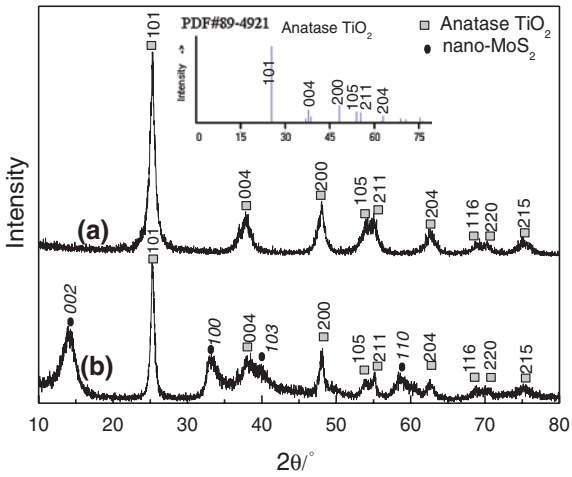

Fig. 10 XRD patterns of: **a** anatase nano-TiO_2 and **b** MoS_2/TiO_2 nanocomposite (adapted from Ref. [35])

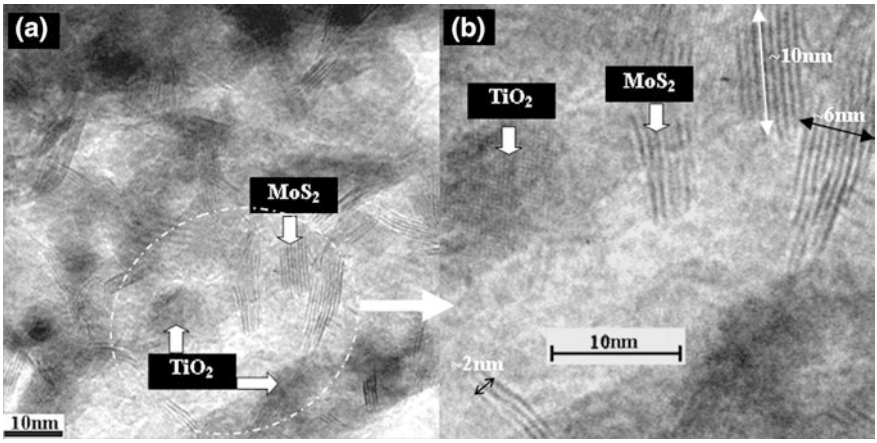

Fig. 11 HRTEM micrographs of the prepared MoS_2/TiO_2 nanocomposite: **a** typical inner region and **b** magnified image of (**a**) (adapted from Ref. [35])

However, the nanoparticles easily agglomerated during the lubrication, leading to inhomogeneous lubrication and asymmetrical furrows (Fig. 13) [23]. Moreover, nano-MoS_2 with the higher chemical activity was more easily reacted with friction pair materials as compared to nano-TiO_2. Thus, the chemical corrosion was also a wear factor of steel balls.

A synergistic effect between nano-TiO_2 and graphite was ascribed to the effective transferring films on friction surfaces and the reinforcing effect of nanoparticles [37]. A transferring film was also found on the steel balls lubricated by the

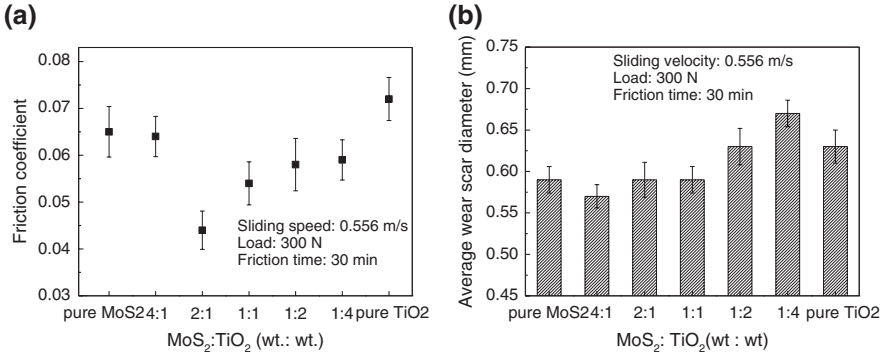

Fig. 12 Tribological properties of MoS_2/TiO_2 nanocomposites: **a** friction coefficient and **b** wear scar diameter (adapted from Ref. [36])

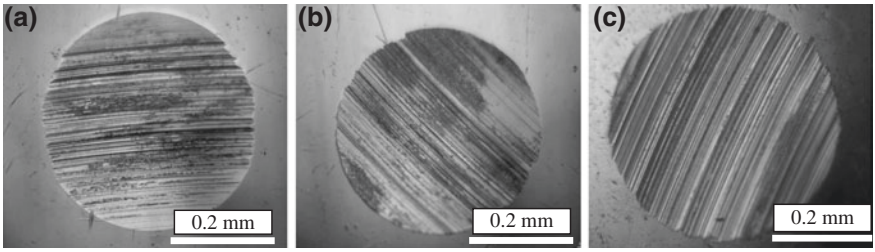

Fig. 13 Optical micrographs of typical wear scars on the bottom balls lubricated by liquid paraffin at 0.556 m/s under 300 N for 30 min with: **a** pure nano-MoS_2, **b** MoS_2/TiO_2 nanocomposite of 4:1, and **c** pure nano-TiO_2 (adapted from Ref. [36])

MoS_2/TiO_2 nanocomposite [36]. The elements Mo and Ti are found in the X-ray photoelectron spectrum (XPS) of the wear scar lubricated by the MoS_2/TiO_2 nanocomposite (Fig. 14) [36]. This implies that MoS_2 and TiO_2 were transferred to the surface of friction pairs from the nanocomposite during friction process. The transfer produced a lubrication film on the steel balls, composed of MoO_3, TiO_2, Fe_2O_3 (or Fe_3O_4), $Fe_2(SO_4)_3$ (or $FeSO_4$), FeS, and carbon-containing compounds after tribochemical reactions.

The excellent lubrication of MoS_2/TiO_2 nanocomposite can also be explained using the effect of nano-TiO_2 on the size and layer distance of nano-MoS_2. Nano-MoS_2 in MoS_2/TiO_2 nanocomposite had smaller thicknesses and larger layer distances as compared to the pure nano-MoS_2. The Large layer distances weakened the Van der Waals force between adjacent MoS_2 molecular layers. Thus, the shearing force needed between these layers decreased. Moreover, the lubrication of the MoS_2/TiO_2 nanocomposite could also be attributed to the micro-cooperation of various nanoparticles with different shapes and lubrication mechanisms [32, 34],

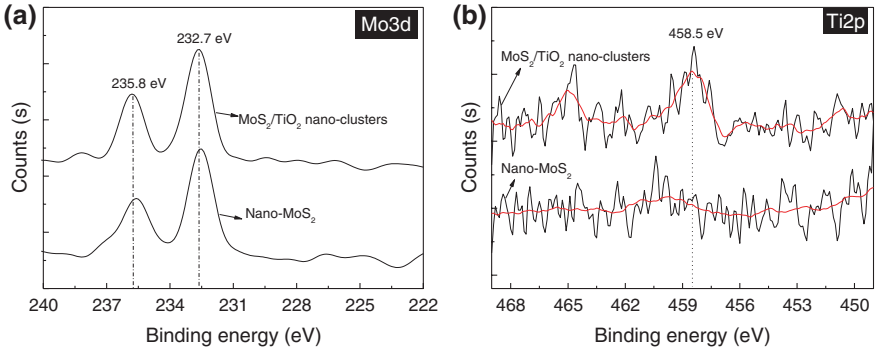

Fig. 14 XPS spectra of wear scars on the top balls lubricated by liquid paraffin at 0.556 m/s under 300 N for 30 min with pure nano-MoS_2 or 2:1 MoS_2/TiO_2 nano-clusters: **a** Mo_{3d} and **b** Ti_{2p} (adapted from Ref. [36])

i.e. the micro-cooperation of MoS_2 nano-platelets and TiO_2 solid nanoparticles during the friction process.

4.3 MoS_2/Polymer Nanocomposites

Mechanically mixing nano-MoS_2 and polymers is the simplest method to prepare MoS_2/polymer nanocomposites for tribological applications. The organic matrix materials mainly included polyoxymethylene (POM) [16, 38–42] and high-density polyethylene (HDPE) [2]. The addition of nano-MoS_2 into polymers had to be done by the heating treatment. It was found that MoS_2 nano-platelet could degrade POM into poisonous formaldehyde in the thermal process (Fig. 15) [16]. Thus, MoS_2 nano-platelet could not be added into POM. Two composites, i.e. MoS_2 micro-platelet/POM and nano-sphere/POM (Fig. 16) [39], were obtained by the mechanical mixing. The nano-sphere/POM revealed better performances in friction reduction and wear resistance as compared to the micro-platelet/POM [40]. Chemical intercalation was an effective chemical method to obtain the MoS_2/POM nanocomposite [3, 42]. The chemical intercalation could disperse MoS_2 better than the mechanical mixing does (Fig. 17) [3]. However, the chmical intercalation destroyed the crystal structure of 2H MoS_2 that is the basis of lubrication. Thus, the intercalation composite did not reveal good lubrication performance (Fig. 18) [40].

HDPE polymer has a more stable structure than POM and the stability of HDPE cannot be affected by nano-platelets at high temperatures [2]. Thus, two nano-MoS_2/HDPE composites, i.e. nano-platelet/HDPE and nano-sphere/HDPE, were prepared by the mechanical mixing (Fig. 19). A fair and interesting comparison was achieved between nano-platelet/HDPE and nano-sphere/HDPE. The

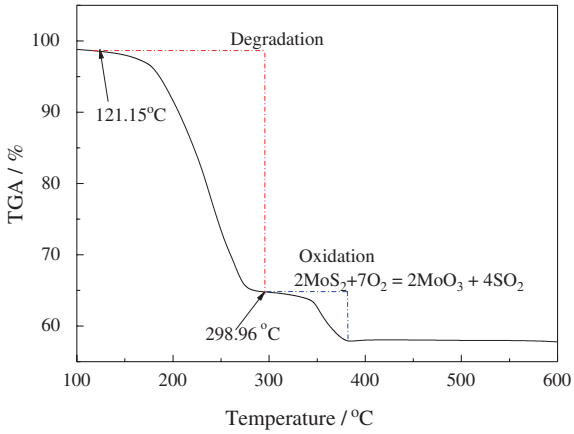

Fig. 15 TGA curve of the mixture of POM powder and MoS_2 nano-platelet (adapted from Ref. [16])

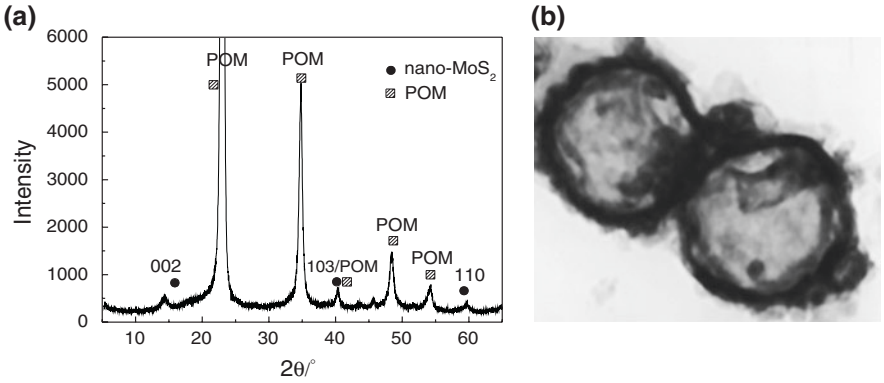

Fig. 16 XRD pattern (**a**) and TEM image (**b**) of POM/MoS_2 nano-sphere composites prepared by mechanical mixing (adapted from Ref. [39])

literature studied the tribological properties at various MoS_2 contents in HDPE from 0.5 to 2.0 wt % under dry friction and oil lubrication, respectively. The results show that the two composites of MoS_2 micro-platelet/HDPE and nano-sphere/HDPE exhibited a similar performance in friction reduction under dry friction. However, the composite with 1.0 wt % MoS_2 nano-platelet showed lower friction coefficients than both micro-platelets/HDPE and nano-spheres/HDPE. The lowest friction coefficient occurred in the composite with 2.0 wt % MoS_2 micro-platelets or nano-spheres (Fig. 20). Under oil lubrication, the nano-sphere/HDPE composite showed the best tribological properties, especially the wear resistance. However, the nano-platelet/HDPE showed no expected tribological properties.

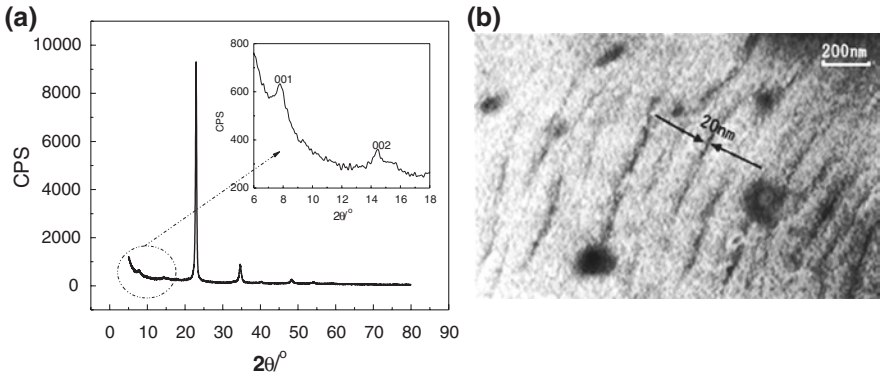

Fig. 17 Intercalation compound of POM/MoS_2: **a** XRD pattern and **b** TEM (adapted from Ref. [3])

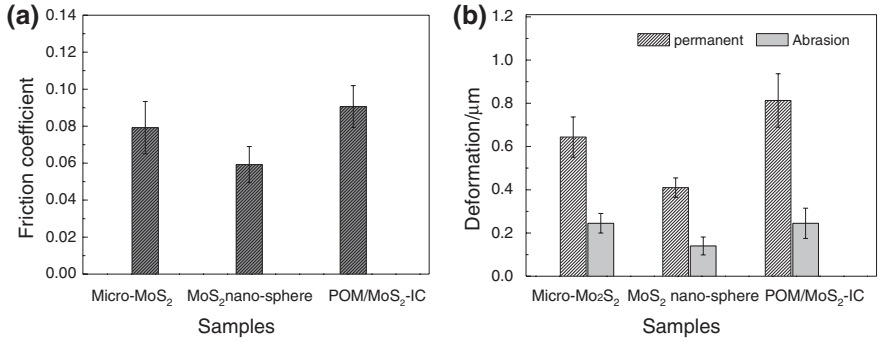

Fig. 18 Tribological properties of MoS_2/POM (IC-intercalation compound) (adapted from Ref. [40])

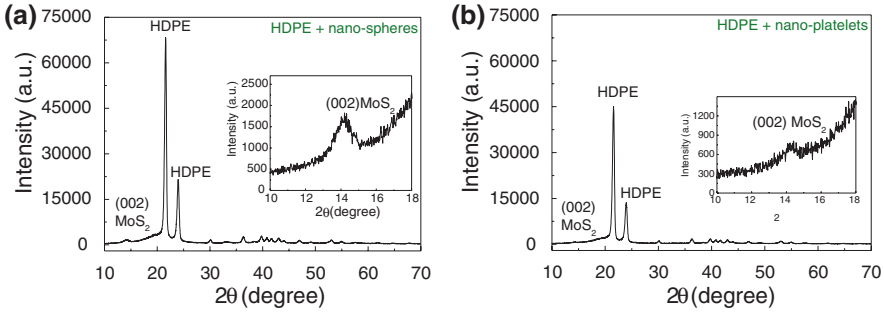

Fig. 19 XRD patterns of: **a** 2.0 % MoS_2 nano-spheres/HDPE and **b** 2.0 % MoS_2 nano-platelets/HDPE (adapted from Ref. [2])

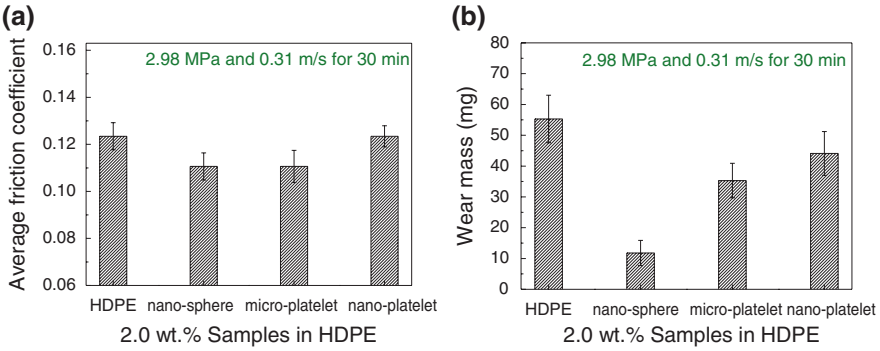

Fig. 20 Tribological properties of MoS_2/HDPE nanocomposites under dry friction: **a** friction coefficient and **b** wear mass (adapted from Ref. [2])

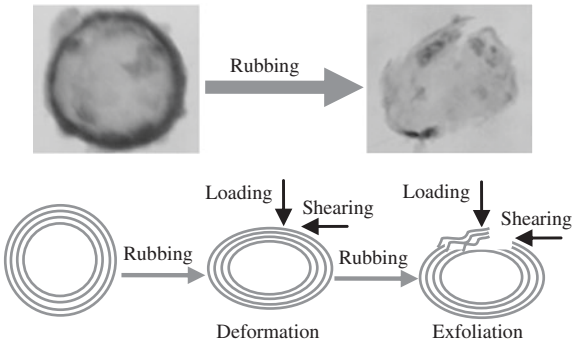

Fig. 21 Schematic diagram of the anti-wear process of MoS_2 nano-sphere (adapted from Ref. [2])

The melting was the main wear mechanism of MoS_2/HDPE composites under dry friction, whereas the abrasive wear became the main wear mechanisms under oil lubrication. The tribological properties of MoS_2/HDPE composites were influenced by their crystallinity and thermo-mechanical behaviors. The addition of nano-sphere into HDPE improved the mechanical behaviors of HDPE, thus leading to better tribological properties. The excellent anti-wear properties of nano-sphere/HDPE composite were attributed to the deformation and exfoliation of the nano-spheres during the friction process (Fig. 21).

4.4 Ni–P–(Nano-MoS_2) Composite Coatings

Ni–P composite coatings with organic or inorganic particles present wide applications in corrosion protection, wear resistance, and friction reduction. Solid lubricants, such as PTFE [43, 44], carbon nanotube [45–47], WS_2 [48], and MoS_2 [49–52], are appropriate additives to modify the Ni–P coatings.

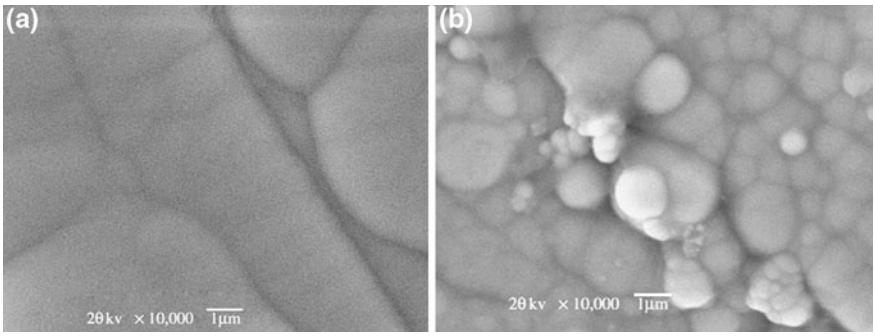

Fig. 22 SEM images of Ni–P electroless coating (**a**) and Ni–P–(nano-MoS_2) electroless coating (**b**) (adapted from Ref. [51])

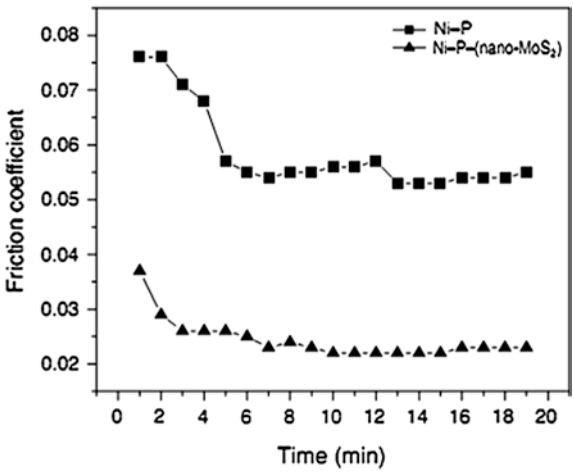

Fig. 23 Friction coefficients of Ni–P and Ni–P–(nano-MoS_2) electroless coatings (adapted from Ref. [51])

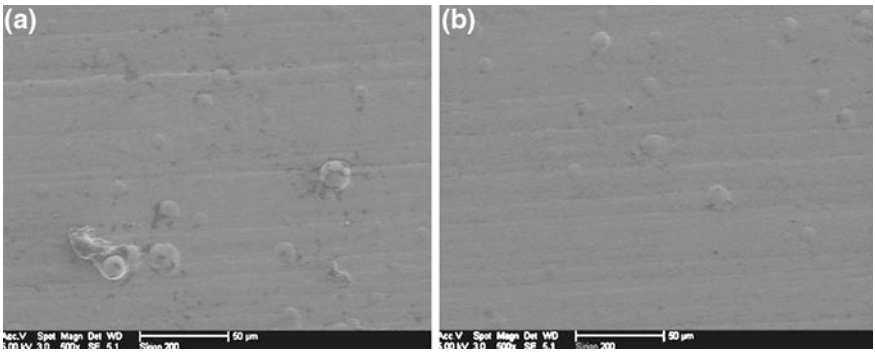

Fig. 24 SEM images of wear surfaces of: Ni–P (**a**) and Ni–P–(nano-MoS_2) (**b**) coatings (adapted from Ref. [51])

Ni–P coatings may be co-deposited with MoS_2 nanoparticles on medium carbon steel substrate by electroless plating [50–52]. Figure 22 shows the SEM images of electroless Ni–P and Ni–P–(nano-MoS_2) composite coatings reported in Ref [51]. The corrosion resistance of the Ni–P–(nano-MoS_2) composite coating was slightly lower than that of the Ni–P coating without MoS_2. As shown in the figure, the cell volume became smaller in the Ni–P–(nano-MoS_2) composite coating as compared to that in the Ni–P coating. It was also found that the nano-MoS_2 particles were around the cell boundary. The Ni–P–(nano-MoS_2) coating showed the super low friction coefficients during the whole rubbing process (Fig. 23). This was attributed to the super lubricity of spherical nano-MoS_2. Moreover, the wear of the Ni–P–(nano-MoS_2) coating was also reduced by the nano-MoS_2 added (Fig. 24).

5 Conclusions

(1) MoS_2-based nanocomposites may be prepared by mechanical mixing, chemical method and electroless coating technology. They usually have better tribological properties than their original materials and play an important role in the lubricating composites.
(2) The chemical method generally reveals advantages over the mechanical one in the preparation of MoS_2 nanocomposites with different morphologies for lubrication applications. However, the chemical intercalation can not improve the tribological properties of MoS_2 nanocomposites, because the intercalation reaction destroys the 2H structure of MoS_2 with better lubrication.
(3) MoS_2/TiO_2 nanocomposite may be prepared by depositing nano-MoS_2 on nano-TiO_2. Nano-MoS_2 and nano-TiO_2 present a positive synergetic effect on the lubrication of the nanocomposite. The sizes of MoS_2 in the nanocomposites are smaller and its layer distances are larger than those of pure nano-MoS_2. Large layer distances weaken the Van der Waals force and small sizes enable MoS_2 to enter the contact region more easily, leading to better anti-friction performance.
(4) Mechanically mixing nano-MoS_2 and polymers, such as POM and HDPE, may produce nano-MoS_2/polymer nanocomposites. MoS_2 nano-sphere in the polymers shows a good lubrication over MoS_2 nano-platelet. The excellent anti-wear properties of nano-spheres are attributed to the deformation and exfoliation of the nano-spheres during the friction process.
(5) Ni–P coatings may be co-deposited with nano-MoS_2 particles on medium carbon steel substrate by electroless plating. The co-deposited nano-MoS_2 significantly improves the friction reduction of Ni–P coating.

Acknowledgments This work was financially supported by the National Natural Science Foundation of China (Grant No. 50905054 and 51275143), China Postdoctoral Science Foundation

funded Project (Grant No. 2011M500110), Foundation of State Key Laboratory of Solid Lubrication (Grant No. 0907), and Talents Foundation of Hefei University (Grant No. 12RC03).

References

1. Benavente E, Santa Ana MA, Mendizábal F, González G (2002) Intercalation chemistry of molybdenum disulfide. Coord Chem Rev 224:87–109
2. Hu KH, Hu XG, Wang J, Xu YF, Han CL (2012) Tribological properties of MoS_2 with different morphologies in high-density polyethylene. Tribol Lett 47:79–90
3. Wang J, Hu KH, Xu YF, Hu XG (2008) Structural, thermal, and tribological properties of intercalated polyoxymethylene/molybdenum disulfide nanocomposites. J Appl Polym Sci 110:91–96
4. Zhang Z, Liu W, Xue Q, Zen J (1998) Current state of tribological application and research of Mo compounds as lubricating materials. Tribology 18(4):377–382
5. Dunckle CG, Aggleton M, Glassman J, Taborek P (2011) Friction of molybdenum disulfide–titanium films under cryogenic vacuum conditions. Tribol Int 44:1819–1826
6. Kalin M, Kogovšek J, Remškar M (2012) Mechanisms and improvements in the friction and wear behavior using MoS_2 nanotubes as potential oil additives. Wear 280–281:36–45
7. Luo J, Zhu MH, Wang YD, Zheng JF, Mo JL (2011) Study on rotational fretting wear of bonded MoS_2 solid lubricant coating prepared on medium carbon steel. Tribol Int 44:1565–1570
8. Feldman Y, Wasserman E, Srolovitz DJ, Tenne R (1995) High rate, gas phase growth of MoS_2 nested inorganic fullerenes and nanotubes. Science 267:222–225
9. Nath M, Govindaraj A, Rao CNR (2001) Simple synthesis of MoS_2 and WS_2 nanotubes. Adv Mater 13:283–286
10. Li XL, Li YD (2004) MoS_2 nanostructures: synthesis and electrochemical Mg^{2+} intercalation. J. Phys Chem B 108:13893–13900
11. Hu KH, Hu XG (2009) Formation, exfoliation and restacking of MoS_2 nanostructures. Mater Sci Technol 25:407–414
12. Hu KH, Wang YR, Hu XG, Wo HZ (2007) Preparation and characterisation of ball-like MoS_2 nanoparticles. Mater Sci Technol 23:242–246
13. Lavayen V, Mirabal N, O'Dwyer C, Santa Ana MA, Benavente E, Sotomayor Torres CM, González G (2007) The formation of nanotubes and nanocoils of molybdenum disulphide. Appl Surf Sci 253:5185–5190
14. Cizaire L, Vacher B, Mogne TL, Martin JM, Rapoport L, Margolin A, Tenne R (2002) Mechanisms of ultra-low friction by hollow inorganic fullerene-like MoS_2 nanoparticles. Surf Coat Technol 160:282–287
15. Rapoport L, Feldman Y, Homyonfer M, Cohen H, Sloan J, Hutchison JL, Tenne R (1999) Inorganic fullerene-like material as additives to lubricants: structure–function relationship. Wear 225–229:975–982
16. Hu KH, Hu XG, Sun XJ (2010) Morphological effect of MoS_2 nanoparticles on catalytic oxidation and vacuum lubrication. Appl Surf Sci 256:2517–2523
17. Rapoport L, Moshkovich A, Perfilyev V, Laikhtman A, Lapsker I, Yadgarov L, Rosentsveig R, Tenne R (2012) High lubricity of re-doped fullerene-like MoS_2 nanoparticles. Tribol Lett 45:257–264
18. Zou TZ, Tu JP, Huang HD, Lai DM, Zhang LL, He DN (2006) Preparation and tribological properties of inorganic fullerene-like MoS_2. Adv Eng Mater 8:289–293
19. Hu KH, Liu M, Wang QJ, Xu YF, Schraube S, Hu XG (2009) Tribological properties of molybdenum disulfide nanosheets by monolayer restacking process as additive in liquid paraffin. Tribol Int 42:33–39
20. Chhowalla M, Amaratunga GAJ (2000) Thin films of fullerene-like MoS_2 nanoparticles with ultra-low friction and wear. Nature 407:164–167

21. Rosentsveig R, Gorodnev A, Feuerstein N, Friedman H, Zak A, Fleischer N, Tannous J, Dassenoy F, Tenne R (2009) Fullerene-like MoS_2 nanoparticles and their tribological behavior. Tribol Lett 36:175–182
22. Rapoport L, Fleischer N, Tenne R (2005) Applications of WS_2 (MoS_2) inorganic nanotubes and fullerene-like nanoparticles for solid lubrication and for structural nanocomposites. J Mater Chem 15:1782–1788
23. Hu KH, Hu XG, Xu YF, Huang F, Liu JS (2010) The effect of morphology on the tribological properties of MoS_2 in liquid paraffin. Tribol Lett 40:155–165
24. Tannous J, Dassenoy F, Lahouij I, Le Mogne T, Vacher B, Bruhács A, Tremel W (2011) Understanding the tribochemical mechanisms of IF-MoS_2 nanoparticles under boundary lubrication. Tribol Lett 41:55–64
25. Lahouij I, Dassenoy F, Vacher B, Martin JM (2012) Real time TEM imaging of compression and shear of single fullerene-like MoS_2 nanoparticle. Tribol Lett 45:131–141
26. Lahouij I, Dassenoy F, de Knoop L, Martin JM, Vacher B (2011) In situ TEM observation of the behavior of an individual fullerene-Like MoS_2 nanoparticle in a dynamic contact. Tribol Lett 42:133–140
27. Daage M, Chianelli RR (1994) Structure-function relations in molybdenum sulfide catalysts: the "rim-edge" model. J Catal 149:414–427
28. Wo HZ, Hu KH, Hu XG (2004) Tribological properties of MoS_2 nanoparticles as additive in a machine oil. Tribology 24:33–37
29. Wang TM, Shao X, Wang QH, Liu WM (2005) Preparation and tribological behavior of polyimide MoS_2 intercalation composite. Tribology 25:322–327
30. Joly-Pottuz L, Martin JM, Dassenoy F, Belin M, Montagnac R, Reynard B (2006) Pressure-induced exfoliation of inorganic fullerene-like WS_2 particles in a Hertzian contact. J Appl Phys 99:023524–023528
31. Tevet O, Goldbart O, Cohen SR, Rosentsveig R, Popovitz-Biro R, Wagner HD, Tenne R (2010) Nanocompression of individual multilayered polyhedral nanoparticles. Nanotechnology 21:365705–365711
32. Hu KH, Cai YK, Hu XG, Xu YF (2010) Synergistic lubrication of MoS_2 particles with different morphologies in liquid paraffin. Ind Lubr Tribol, Ref: ilt-10-2010-0075, accepted manuscript
33. Hu KH, Hu XG, Jiang P (2010) Large-scale and morphology-controlled synthesis of nano-sized molybdenum disulphide particles by different sulphur sources. Int J Mater Prod Technol 39:378–387
34. Hu KH, Cai YK, Hu XG, Xu YF (2011) Synthesis and tribological properties of MoS_2 composite nanoparticles with different morphologies. Surf Eng 27:544–550
35. Hu KH, Hu XG, Xu YF, Sun JD (2010) Synthesis of nano-MoS_2/TiO_2 composite and its catalytic degradation effect on methyl orange. J Mater Sci 45:2640–2648
36. Hu KH, Huang F, Hu XG, Xu YF, Zhou YQ (2011) Synergistic effect of nano-MoS_2 and anatase nano-TiO_2 on the lubrication properties of MoS_2/TiO_2 nano-clusters. Tribol Lett 43:77–87
37. Xian G, Walter R, Haupert F (2006) A synergistic effect of nano-TiO_2 and graphite on the tribological performance of epoxy matrix composites. J Appl Polym Sci 102:2391–2400
38. Hu KH, Wang J, Schraube S, Xu YF, Hu XG, Stengler R (2009) Tribological properties of MoS_2 nano-balls as filler in plastic layer of three-layer self-lubrication bearing materials. Wear 266:1198–1207
39. Hu KH, Sun XJ, Xu YF, Salomon M, Hu XG (2009) Tribological properties of POM-based self-lubrication composites with MoS_2 in vacuum. J Hefei Univ Technol 32:615–619
40. Hu KH, Schraube S, Xu YF, Hu XG, Stengler R (2010) Micro-tribological behavior of polyacetal-based self-Lubrication composite materials modified with MoS_2. Tribology 30:38–45
41. Hu X, Hu K, Sun X, Xu Y (2010) Space tribological properties of MoS_2-based self-lubrication composite materials. Spacecraft Environ Eng 27(1):50–53
42. Hu KH, Xu YF, Wang J, Hu XG, Schraube S, Stengler R (2007) Tribological behavior of self-lubrication bearing materials of steel-copper-polyoxymethylene containing MoS_2-IC nanoparticles. ASME/STLE 2007 international joint tribology conference (IJTC2007), 2007, San Diego, California, USA, pp 787–789

43. Ramalho A, Miranda JC (2005) Friction and wear of electroless NiP and NiP + PTFE coatings. Wear 259:828–834
44. Rossi S, Chini F, Straffelini G, Bonora PL, Stampali A (2003) Corrosion protection of electroless nickel/PTFE, phos-phate/MoS_2 and bronze/PTFE coatings applied to improvethe wear resistance of carbon steel. Surf Coat Technol 173:235–242
45. Chen WX, Tu JP, Xu ZD, Chen WL, Zhang XB, Cheng DH (2003) Tribological properties of Ni-P-multi-walled carbon nanotubes electroless composite coating. Mater Lett 57:1256–1260
46. Wang LY, Tu JP, Chen WX, Wang YC, Liu XK, Olk C, Cheng DH, Zhang XB (2003) Friction and wear behavior of electroless Ni-based CNT composite coatings. Wear 254:1289–1293
47. Chen XH, Chen CS, Xiao HN, Cheng FQ, Zhang G, Yi GJ (2005) Corrosion behavior of carbon nanotubes-Ni composite coating. Surf Coat Technol 191:351–356
48. Chen WX, Tu JP, Ma XC, Xu ZD, Chen WL, Wang JG, Cheng DH, Xia JB, Gan HY, Jin YX, Tenne R, Rosenstveig R (2002) Preparation and tribological properties of Ni-P electroless composite coating containing inorganic fullerene-Like WS_2 nanomaterials. Acta Chim Sin 60:1722–1726
49. Zou TZ, Tu JP, Zhang SC, Chen LM, Wang Q, Zhang LL, He DN (2006) Friction and wear properties of electroless Ni-P- (IF-MoS_2) composite coatings in humid air and vacuum. Mater Sci Eng, A 426:162–168
50. Hu XG, Cai WJ, Xu YF, Wan JC, Sun XJ (2009) Electroless Ni–P–(nano-MoS_2) composite coatings and their corrosion properties. Surf Eng 25:361–366
51. Hu X, Jiang P, Wan J, Xu Y, Sun X (2009) Study of corrosion and friction reduction of electroless Ni–P coating with molybdenum disulfide nanoparticles. J Coat Technol Res 6:275–281
52. Hu XG, Cai WJ, Wan JC, Xu YF, Sun XJ. Study of corrosion performance of electroless Ni-P coating with molybdenum disulfide nanoparticles. Key Eng Mater 373–374:256